

## Research Article

# Analysis of Flexural Buckling Capacity of Stainless Steel Columns under Axial Compression

Yong Liang <sup>1</sup>, Gapi Shu <sup>2</sup>, and Shaohua Li <sup>3</sup>

<sup>1</sup>Jiaxing Nanyang Polytechnic Institute, Jiaxing, China

<sup>2</sup>Jiaxing Nanyang Polytechnic Institute, Shanghai 200092, China

<sup>3</sup>China Jovan Holding Group Co Ltd, Hong Kong, China

Correspondence should be addressed to Yong Liang; [stepinnewage@126.com](mailto:stepinnewage@126.com)

Received 19 April 2022; Revised 1 August 2022; Accepted 5 August 2022; Published 5 September 2022

Academic Editor: Krishanu Roy

Copyright © 2022 Yong Liang et al. This is an open access article distributed under the Creative Commons Attribution License, which permits unrestricted use, distribution, and reproduction in any medium, provided the original work is properly cited.

In order to provide a basis for the compilation of the bending buckling stability part of axially compressed columns in the technical code for stainless steel structures, the design methods and experimental research data of similar components are collected and compared. The results showed that there are some deficiencies in the current European code for the design of stainless steel structures and the American code for the design of cold-formed stainless steel structures. According to the collected test data of square tube, rectangular tube, circular tube, elliptical tube, welded H-shaped steel, and cold-formed C-shaped steel for 199 section columns and according to the influence of cold-formed effect and residual stress on the stability of axial compression members, the members are divided into three categories: A, B, and C according to the section form, in which the columns with cold-formed square, rectangular hollow section, and lipped C-section were included in A, columns with circular and oval hollow section were sorted into B, columns with welded H-section were separated into C, and the three categories of axial compression stability curves are expressed in the form of Perry formula. The comparison with the test data shows that the three kinds of curves can well estimate the stability bearing capacity of members, and the discreteness is small. The reliability of the proposed formula is analyzed, and the results show that its reliability index  $\beta$  meets the requirements of the GB 50068 standard.

## 1. Introduction

The output of stainless steel has increased rapidly in recent years, and the application range of stainless steel materials has gradually expanded from traditional decorative components to structural load-bearing components in the construction industry. The mechanical properties of stainless steel are quite different from ordinary low-carbon steel [1], and the design expression of stainless steel components is also quite different from ordinary low-carbon steel. With the wide application of stainless steel structural members, the design method of stainless steel structural members has become the focus of researchers and designers.

Scholars have conducted a large number of experimental studies on stainless steel components from 1990 to 2021 [2–26], and put forward a variety of design methods for stainless steel components [21, 27–30]. These stainless steel

components include cold-formed square pipe, rectangular pipe, round pipe, welded H-shaped steel, cold-formed C-shaped steel, and double C-shaped steel, covering the commonly used stainless steel section types. The materials of components include common 304 stainless steel, 316 stainless steel, high strength stainless steel (HSA), and duplex stainless steel. The range of mechanical properties of the material is  $\sigma_{0.2} \in [241, 942]$  MPa, hardening index  $n \in [3.0, 13.75]$ , covering the range of mechanical properties of stainless steel materials for construction. The buckling behavior of stainless steel components includes both single thin-walled structural members and built-up members. The failure modes of components include local buckling, flexural buckling, local buckling and flexural buckling, and distortional buckling, including the common instability forms of biaxial symmetric members. However, the expressions in these design methods of stainless steel components either

ignore the characteristics of stainless steel and directly follow the practice of the low carbon steel, resulting in low calculation accuracy, or take full account of the characteristics of stainless steel, resulting in redundant design expressions.

In order to obtain an accurate and practical design expression for the bending buckling of the stainless steel axial compression columns, this paper first analyzes the existing design methods of stainless steel axial compression members at home and abroad, compares various methods combined with the current structural design characteristics, and selects a method in line with the habits of designers. Then, the test data of axial compression members at home and abroad are collected, and the design expression of bending buckling of stainless steel axial compression columns is fitted through the analysis of the stability characteristics of the stainless steel members; finally, the reliability of the proposed method is analyzed according to the unified standard for reliability design of building structures (GB 50068-2001) [31].

## 2. Existing Design Methods

The representative design methods of stainless steel axial compression columns can be divided into three categories: the first category is Perry method design expression represented by the European code EN1993-1-4 (hereinafter referred to as "European code") for design of stainless steel structures [27]. The second category is the design expression of tangent modulus method represented by the American cold SEI/ASCE 8-02 (hereinafter referred to as "American code") formed stainless steel structure design code [28]. The third category is represented by the member design expression considering the variation in stainless steel material parameters (hereinafter referred to as "K&R method") given by Rasmussen and Rondal [29].

*2.1. The First Type of Design Method.* Perry method has been used in European code to calculate the stable bearing capacity of stainless steel axial compression members, and its stability coefficient  $\chi$  (equivalent to the stability coefficient in Chinese specifications  $\varphi$ ) can be expressed with the following equations:

$$\chi = \frac{1}{\varphi + \sqrt{\varphi^2 - \lambda^2}} \leq 1, \quad (1)$$

$$\varphi = 0.5[1 + \alpha(\lambda - \lambda_0) + \lambda^2], \quad (2)$$

where  $\lambda$  is the normalized slenderness ratio of compression members;  $\alpha$  is the calculation parameter related to the defect (mainly refers to geometric defects and mechanical defects, such as initial bending and residual stress of the structure); and  $\lambda_0$  is the lower limit of regularization slenderness ratio. The value of  $\alpha$  and  $\lambda_0$  varies with the member section type and forming mode.

The design expression of stainless steel members in the European code is the same as that of low-carbon steel members, and is also similar to the design method in China's

GB 50018-2002 technical code for cold-formed thin-wall steel structures [32] and GB50017-2003 code for design of the steel structures [33]. This method does not explicitly reflect the influence of material nonlinearity on the stable bearing capacity of compression members, but by adjusting the defect correlation coefficient ( $\alpha$  and  $\lambda_0$ ) to reflect the influence of material nonlinearity on the stable bearing capacity of compression members.

*2.2. The Second Type of Design Method.* The second type of design method includes the method adopted in American code and Hradil et al. [30].

The calculation method of critical stress for flexural buckling of the compression members in American code is shown in

$$F_n = \frac{\pi^2 E_t}{(KL/r)^2} \leq F_y, \quad (3)$$

where  $F_n$  is the critical stress of the member;  $E_t$  is the tangent elastic modulus corresponding to the critical stress;  $K$  is the effective length coefficient of the member;  $L$  is the geometric length of the member;  $r$  is the radius of gyration of the member section; and  $F_y$  is the nominal yield stress of the material ( $\sigma_{0.2}$ ).

In the American specification, the change in mechanical property parameters of stainless steel materials is considered through the tangent elastic modulus  $E_b$ , the tangent elastic modulus  $E_t$  needs to be calculated back according to the calculated critical stress in the calculation process, and the calculation process needs iteration.

Hradil et al. [30] have considered that the influence of geometric defects on the stability of stainless steel axial compression members was ignored in the design of stainless steel axial compression members according to the tangent modulus method in the American code, and suggested replacing the Euler critical force calculated in the American code with the Perry method in the European code to recalculate the stability coefficient of the members. In this way, the influence of stainless steel material nonlinearity and geometric nonlinearity is considered in the design method of components. The calculation process requires iteration.

Adopting the second type of design method means that iteration must be carried out in the component design, while China's relevant stainless steel material standards [33, 34] only give the initial elastic modulus  $E_0$  and nominal yield strength  $\sigma_{0.2}$  of stainless steel materials, it is necessary to further obtain the hardening exponent  $n$  and constitutive relationship of materials before iterative calculation.

*2.3. The Third Type of Design Method.* The third type of design method includes the K&R method [28] and the method proposed by Zheng [22].

Through finite-element analysis, Rasmussen and Rondal [29] found that the change in mechanical parameters of stainless steel short columns has a great impact on the stable bearing capacity of compression members, and conducted a detailed analysis of this impact, established the stability

curves of nominal yield strength  $\sigma_{0.2}$ , and hardening index  $n$  facing short columns. Reference [28] also proposed to introduce the material mechanical parameters of stainless steel short columns into the defect coefficient expression of Perry method to solve the problem that the stability coefficient of stainless steel compression members changes with the material mechanical parameters. The expression of the defect coefficient is shown as follows:

$$\eta = a[\lambda - \lambda_1]^b - \lambda_0, \quad (4)$$

where  $\eta$  is the defect coefficient of axial compression member;  $a$ ,  $b$ ,  $\lambda_1$ , and  $\lambda_0$  are the functions of three parameters  $E_0$ ,  $\sigma_{0.2}$ , and  $n$  in the Ramberg–Osgood constitutive model of stainless steel.

K&R method forms a stable bearing capacity network in the variation space of main mechanical parameters of materials and geometric parameters of components, covering the range of common material parameters and component geometric parameters. It can be used not only for stainless steel but also for other materials that can be expressed by Ramberg–Osgood constitutive model.

Zheng [22] proposed the concept of modified regularized slenderness ratio by using the derivation idea of K&R method, and fitted the expression of modified regularized slenderness ratio by using the constitutive relationship expression of stainless steel proposed by Fernando et al. [35], considering the overall defect of  $L/1000$ , and substituted the fitting results into Perry method to calculate the stability coefficient of components.

The third design method is based on the material mechanical property parameters of axially compressed short columns, it is considered that the material mechanical properties obtained by short column test include the effects of residual stress and material hardening in corner area, and the accuracy is the best among various methods at present. However, there are obvious shortcomings in this method: (1) the performance of short columns must be obtained before structural calculation, which restricts the flexibility of design. Although this method has high precision, it is still difficult to be applied to design practice; and (2) when dealing with thin-walled members, it is difficult to obtain the parameters of the section average material constitutive model (Ramberg–Osgood equation parameters) by short column test [3], which limits the application scope of this method.

### 3. Analysis and Literature Review of Test Data

**3.1. Literature Review of the Test Data.** So far, researchers have carried out a large number of experimental studies on stainless steel axial compression members. The test data collected in this paper are given in Table 1. These stainless steel components include commonly used stainless steel section types and different types of stainless steel, covering the range of mechanical properties of stainless steel materials for construction, including the common instability forms of biaxial symmetric components. In total, there are 116 short columns and 342 long columns, of which there are 199 members with bending buckling (effective

component). The test data will be used as a database to establish the design method of stainless steel axial compression members.

**3.2. Filter and Analysis of the Test Data.** The purpose of the test data analysis is to separate the members with flexural buckling failure from the test data, and to provide the basis for the bending buckling design formula. In local buckling, flexural buckling, local and flexural buckling, and distorted buckling, it is not easy to distinguish between flexural buckling and local buckling and flexural buckling. In the European code, the section classification method is used to distinguish the two failure forms, the sections are divided into four categories in the code, in which the sections of categories 1–3 do not have a local failure when the overall failure of the member occurs. Gardner and Theofanous [36] studied the section classification in the European code and compared the test data (including stiffened plates and nonstiffened plates) with the section classification in the European code. The comparison shows that the section classification requirements specified in the current European code are too strict, that is, the sections of categories 1–3 can ensure that there is no local buckling before the overall buckling. In this paper, the section classification method of European code is used to analyze the test data to ensure that the selected members have flexural buckling failure. The lower limit values of category 3 sections in the European code are shown in Table 2, in which

$$\varepsilon = \sqrt{\frac{235}{\sigma_{0.2}} \cdot \frac{E_0}{2.1 \times 10^5}}. \quad (5)$$

Where  $E_0$  and  $\sigma_{0.2}$  are taken from the material tensile test. Since there is no division basis for section classification of elliptical section members, the division basis of the circular tube is adopted in this paper, in which  $D$  is the length of the long axis of the ellipse [27].

According to the above analysis basis and the calculation of material mechanical property parameters of member tensile test, there are 41 square tube members, 27 rectangular tube members, 62 circular tube members, 19 welded H-shaped members (including 9 weak axis instability and 10 strong axis instability), 6 elliptical members, and 44 crimped C-steel members. A total of 199 members belong to categories 1–3 sections, all of which have flexural buckling failure.

### 4. Comparative Analysis and Column Curve

**4.1. Comparison of Test Data.** When calculating the flexural buckling of axial compression members in Eurocode, three stability curves are given according to the section forming method. The section types and parameter values corresponding to the three curves are shown in Table 3. Figures 1 and 2 show the comparison of the test data, Eurocode stability curve, and stability curves (class A, class B, and class C) proposed in this paper. In the calculation, the material parameters adopt the plate tensile test data, the section properties of the members adopt the section parameters actually measured in the test, and the partial coefficient of resistance  $\gamma_{M0}$  is taken as 1.0.

TABLE 1: Test data statistics of the stainless steel column.

Year	Reference	Stainless steel grade	Connection mode	Cross section	Number of long columns	Number of short columns	Number of effective components
1992	[2]	304L	Hinge joint	Square tube	6	2	6
				Round tube	8	2	8
1995	[3]	1.4031 (304)	Hinge joint	Square tube	3	1	3
		1.4031 (304)		Rectangular tube	6	2	3
1995	[4]	3Cr <sub>12</sub>	Hinge joint	Welded H-tube	15	—	0
1995	[5]	0Cr <sub>19</sub> Ni <sub>9</sub>	Hinge joint	Round tube	27	0	27
2000	[6]	304	Hinge joint	Cold formed C-tube	44	0	44
2000	[7]	1.4031 (304)/ 1.4462 (2205)	Hinge joint	Welded H-tube	15	0	12
2000	[8]	1.4541 (321)/ 1.4435 (316)	Hinge joint	Round tube	6	3	5
2002	[9]	304	Rigid joint	Round tube	12	4	12
2003, 2004	[10, 11]	304	Hinge joint	Square tube	8	17	5
2003, 2004	[10, 11]	304	Hinge joint	Rectangular tube	14	10	8
2003, 2004	[10, 11]	304	Hinge joint	Round tube	0	4	0
2004	[12]	304	Rigid joint	Square tube	8	4	4
2006	[13]	304	Rigid joint	Rectangular tube	8	16	8
2008	[14]	HAS	Rigid joint	Square tube	—	3	0
2009	[15]	304, 430, 3Cr <sub>12</sub>	Rigid joint	Cold formed C-tube	19	14	0
2010	[16]	Dual phase steel	Rigid joint	Square tube	12	4	7
2010	[16]	1.4318 (301LN)	Rigid joint	Rectangular tube	6	2	0
2012	[17]	1.4318	Hinge joint	Square tube	12	—	6
2014	[18]	304, 404	Hinge joint	Double C-section steel	24	0	0
2014	[18]	304, 430, 3Cr <sub>12</sub>	Hinge joint	Cold formed C-tube	36	0	0
2016	[19]	1.4162	Hinge joint	Square tube	6	6	6
2016	[19]	1.4162	Hinge joint	Rectangular tube	6	2	6
2018	[20]	1.4401 (316)	Hinge joint	Elliptical tube	6	6	6
2019	[21]	304	Hinge joint	Square tube	6	4	4
2020	[22]	304	Hinge joint	Rectangular tube	11	3	2
2021	[23]	304	Hinge joint	Round tube	11	5	10

TABLE 2: Lower limit for sections of class 3 in the European code [36].

Plate type	Sketch map	Limit value
Stiffened elements		$W/t = 30.7\epsilon$
Unstiffened elements		Cold rolling: $W/t = 11.9\epsilon$ welding: $W/t = 11.0\epsilon$
Round tube		$D/t = 90\epsilon^2$

TABLE 3: Parameters for Perry method in Eurocode.

Buckling modes	Section type	$\alpha$	$\lambda_0$		
Flexural buckling	Cold-formed open section (Figure 1)	0.49	0.40		
	Hollow section (welded or rolled, Figure 1)				
	Welded open section (strong axis, Figure 2)			0.49	0.20
	Welded open section (weak axis, Figure 2)			0.76	0.20

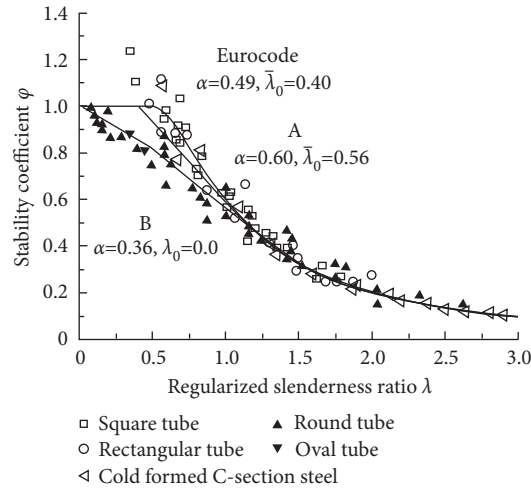


FIGURE 1: Strength curves in Eurocode and the proposed strength curves for A and B.

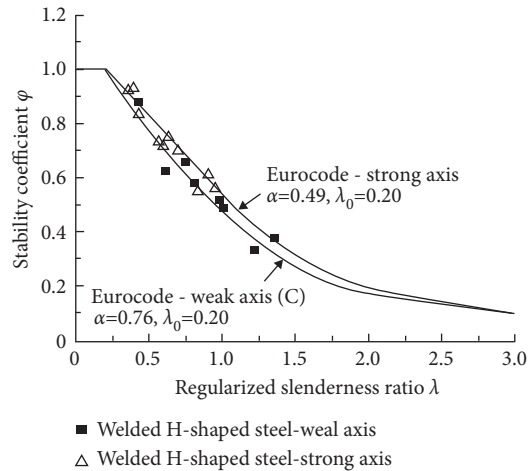


FIGURE 2: Strength curves in Eurocode and proposed strength curve for C.

As can be seen from Figures 1 and 2,

- (1) For the stability curves of closed section and cold-formed open section in European code, when the regularized slenderness ratio  $\lambda \geq 1.25$ , the stability curve is in good agreement with the test data, and when regularized slenderness ratio  $\lambda < 1.25$ , this stability curve is higher than the test value of circular tube members and lower than the test value of square tube, rectangular tube, and cold-formed C-steel members. Stainless steel has high cold working sensitivity, the strength of materials in the corner area of square, rectangular tubes, and cold-formed C-steel members is significantly higher than that in

the flat area, while the material strength distribution on the section of circular tube members is relatively uniform. Therefore, when the stability coefficient is calculated according to the mechanical properties of materials obtained from the tensile test of standard specimens, the calculated value of the component with cold working corner area must be higher than that of the circular tube component, and this trend is more obvious with the decrease in the normalized slenderness ratio of the component.

- (2) The stability curve of welded H-shaped steel members in the European code adopts the curve of welded H-shaped steel members of low carbon steel

compression members [27, 37]. Considering the influence of residual stress on the stability bearing capacity of different buckling axes of welded H-shaped steel members, the stability curve is divided into the strong axis and weak axis. However, it can be seen from the current test data of stainless-steel-welded H-shaped steel members (Figure 2) that there is no significant difference between the strong axis and weak axis test data of welded H-shaped steel, and the test data are lower than the strong axis stability curve. In the current test data, the plate cutting and blanking methods of stainless-steel-welded H-shaped steel members are mostly plate shears; this blanking method produces a certain cold working effect on the edge of the plate, making the material strength of the edge of the plate higher than that of the middle part [23], which weakens the influence of residual stress on the weak axis buckling stability bearing capacity of welded H-shaped members to a certain extent.

**4.2. Recommended Stability Curve.** According to the analysis of the test data, three stability curves are proposed for the design of stainless steel axial compression members. Among them, the cold-formed section (square, rectangular pipe, and C-section steel) members greatly affected by cold processing adopt class A curve, and the stability coefficient of this kind of member is the highest under the same slenderness ratio. Cold-formed circular pipe and elliptical pipe components adopt class B curve, which is reduced when the slenderness ratio is small compared with class A curve. Due to the influence of welding residual stress on welded H-shaped steel members (strong axis and weak axis), the stability curve (class C curve) corresponding to the weak axis of welded H-shaped steel members in European code is adopted.

The least square method is used to fit the test data, and the parameter values of the stability curve are obtained. Table 4 shows the values of parameters for proposed curves and comparison results. The comparison between the three stability curves and the test data is shown in Figures 1 and 2.

As can be seen from Table 4 and Figures 1 and 2, compared with the stability curve in the European code, the design curve proposed in this paper is in good agreement with the test data, the test value is slightly higher than the value of the stability curve, and has less discreteness.

## 5. Reliability Analysis

The unified standard for reliability design of building structures (GB 50068-2001) proposes to use the first-order second-moment method for reliability analysis, and it is also stipulated that for the secondary ductile structures, the reliability index  $\beta \geq 3.2$ . In the GB 50068-2001, the reliability of structural members should be measured by the reliability index. The reliability index of structural members should be calculated by the first-order and second-order matrix method considering the probability distribution type of basic variables. When there are only two basic variables,

action effect, and structural resistance, which are normally distributed, the reliability index of structural members can be calculated according to the following formula:

$$\beta = \frac{\mu_R - \mu_S}{\sqrt{\sigma_R^2 + \sigma_S^2}}, \quad (6)$$

where  $\beta$  is the reliability index of structural members,  $\mu_s$  and  $\sigma_s$  are the average value and standard deviation of the action effect of structural members, and  $\mu_R$  and  $\sigma_R$  are the average value and standard deviation of resistance of structural members.

The load modes of stainless steel structure and ordinary structure are the same, so the same statistical parameters of load random variables can be used. The load statistical parameters used in this paper are shown in Table 5 [37].

The resistance of members is affected by the uncertainty of the material's strength, geometric parameters, and calculation mode. Li et al.[38] suggested that the strength standard value of stainless steel materials should be 201 MPa to 205 MPa, according to the test data of stainless steel specimens. The strength uncertainties of corresponding stainless steel materials of the 0Cr<sub>18</sub>Ni<sub>9</sub>, 1Cr<sub>18</sub>Ni<sub>9</sub>, and 00Cr<sub>18</sub>Ni<sub>9</sub> are as follows:  $\mu_1 = 1.366$ ,  $\delta_1 = 0.050$  9;  $\mu_2 = 1.257$ ,  $\delta_2 = 0.067$  8;  $\mu_3 = 1.322$ , and  $\delta_3 = 0.051$  5. The test data collected in this paper include a variety of stainless steel materials, which have great differences in material strength, and lack corresponding material strength statistics. According to the results of reference [39], based on the principle of conservatism, the statistical parameters of material strength adopted in this paper are as follows:  $\mu_m = 1.200$  and  $\delta_m = 0.070$ . Referring to the statistical results of steel members in China, the uncertainty of geometric parameters of members is taken as  $\mu_a = 1.00$ ,  $\delta_a = 0.050$ . According to the limit theorem of the probability center, the resistance of members will approximately conform to lognormal distribution. The statistical parameters of the three stability curves calculated by the above method are shown in Table 6.

Referring to the provisions on structural load combination in load code for building structures (GB 50009-2001) [38], this paper calculates a combination with variable load and considering the control effect of dead load. The load combinations used in reliability analysis are shown in Table 7. The partial coefficient  $\gamma_R$  of resistance under a limited state of bearing capacity is taken as 1.15 [39].

In the reliability analysis of components, the ratio  $\rho$  of the standard value of live load effect and the standard value of dead load effect has a great impact on the analysis results; according to the load ratio that often occurs in engineering, this paper considers that  $\rho$  take 0.25, 0.50, 1.00, 2.00, and 4.00.

According to the values of the above parameters, the reliability index  $\beta$  calculated by the checkpoint method (JC method) is shown in Table 8, and compared with the traditional method for solving complex transcendental equations, this method has the characteristics of not easy divergence, fast convergence speed, and high accuracy of calculation results [40]. Among them, when  $\rho$  takes 0.25 and 0.50, the combination of dead load control is adopted; and when  $\rho$  takes other values (1.00, 2.00, and 4.00), the combination of live load control is adopted.

TABLE 4: Values of parameters for proposed curves and comparison results.

Flexion pattern	Section type	$\alpha$	$\lambda$	Mean value	Standard deviation
Bending buckling	Cold formed	0.60	0.56	1.024	0.095
	Round tube	0.36	0.00	1.020	0.105
	Welded H-shape	0.76	0.20	1.050	0.076

TABLE 5: Statistical parameters of external load.

Load type	Mean value/standard value	Coefficient of variation	Distribution type
Dead load	1.060	0.070	Normal distribution
Live load (residential)	0.644	0.230	Extreme value I-type distribution
Live load (office)	0.524	0.288	Extreme value I-type distribution
Wind load	0.908	0.193	Extreme value I-type distribution

TABLE 6: Resistance variation in strength curves.

Stability curve	Mean value	Coefficient of variation	Distribution type
A	1.228 8	0.126 5	Lognormal distribution
B	1.224 0	0.134 2	Lognormal distribution
C	1.260 0	0.112 4	Lognormal distribution

TABLE 7: Load combinations.

Number	Dead load control	Live load control
Combination 1	1.35 dead load + 1.4 × 0.7 live load (residential)	1.2 dead load + 1.4 live load (residential)
Combination 2	1.35 dead load + 1.4 × 0.7 live load (office)	1.2 dead load + 1.4 live load (office)
Combination 3	1.35 dead load + 1.4 × 0.6 wind load	1.2 dead load + 1.4 wind load

TABLE 8: Calculated results of the reliability index  $\beta$ .

Load combination		$\beta$					Mean value
		$\rho = 0.25$	$\rho = 0.50$	$\rho = 1.00$	$\rho = 2.00$	$\rho = 4.00$	
Class A stability curve	Combination 1	4.30	4.21	4.36	4.22	4.11	4.24
	Combination 2	4.45	4.40	4.55	4.41	4.31	4.42
	Combination 3	3.78	3.36	3.63	3.44	3.30	3.50
Class B stability curve	Combination 1	4.07	4.03	4.24	4.13	4.04	4.10
	Combination 2	4.22	4.23	4.43	4.33	4.24	4.29
	Combination 3	3.56	3.21	3.52	3.36	3.23	3.38
Class C stability curve	Combination 1	4.91	4.66	4.67	4.46	4.31	4.60
	Combination 2	5.07	4.83	4.84	4.63	4.49	4.77
	Combination 3	4.34	3.77	3.92	3.66	3.49	3.84

As can be seen from Table 8, the reliability indexes  $\beta$  of the three stability curves proposed in this paper are all greater than 3.2, and meet the requirements of relevant specifications. The reliability index of class C stability curve is the highest, followed by class A, and class B is the lowest. Among all kinds of load combinations, the combination reliability index of wind load is the lowest [41, 42].

## 6. Conclusion

The design indexes and uncertain statistics of stainless steel materials have a great impact on the accuracy of component design methods. At present, the statistical data of design indexes of stainless steel materials are not perfect and need to be further studied. By collecting and comparing the existing design methods and experimental research data of similar components, the following conclusions are obtained:

- (1) Compared with the design method of axial compression members proposed by the current American code and foreign scholars, the design method of axial compression members in the current European code is simpler, but it is not reasonable to divide the round tube, square tube, and rectangular tube members into one category in its stability curve classification.
- (2) The section classification method of European code is used to screen the test data so as to separate the members with flexural buckling failure from the test data as the basis for the flexural buckling design formula, and a total of 199 members belong to categories 1–3 sections, all of which have flexural buckling failure.
- (3) The stainless steel members are divided into three types according to the forming mode and section form, the stability curves of the three types of

members are fitted by Perry method, and the stability curves are in good agreement with the experimental data. The stability curve of the three types of members can better estimate the stability bearing capacity of members, and the discreteness is small.

- (4) The reliability analysis of the three stability curves shows that the reliability indexes of the three stability curves are greater than 3.2.

## Data Availability

The data used to support the findings of this study are available from the corresponding author upon request in the e-mail address: stepinnewage@126.com link to the Institutional web page of the corresponding author: <https://www.jxny.net>. The underlying data supporting the results of this study can be found in previous publications for the mentioned authors. List of the previous publications are as follows: (1) Liang Yong and Zhang Han. Research and Analysis on section classification method of stainless steel pipe based on plate correlation[J]. Theoretical research on urban construction, 2019(26):41–42(In Chinese). (2) Liang Yong, Gao Gao, Zhang Mengxi, et al. Model test of Geocell Reinforced Embankment under graded cyclic load [J] Geotechnical mechanics, 2016, 37 (8): 2213–22210 (In Chinese). et al. please link to: <https://www.cnki.net>, where you can find the detail. All the authors listed have approved the manuscript that is enclosed.

## Conflicts of Interest

The authors declare that they have no conflicts of interest.

## Acknowledgments

This work was supported by the Key Industrialization Projects of the 14th Five-Year Plan of Zhejiang Provincial Department of Education (JJKH20201242KJ) and National Natural Science Foundation of China (51178109).

## References

- [1] X. Chang and H. G. Lei, "Research progress and review of stainless steel civil architecture," *IOP Conference Series: Earth and Environmental Science*, vol. 647, no. 1, pp. 12200–12211, 2021.
- [2] K. J. R. Rasmussen and G. J. Hancock, "Design of Cold-formed stainless steel tubular members. I: Columns," *Journal of Structural Engineering*, vol. 119, no. 8, pp. 2349–2367, 1993.
- [3] A. Tajia and P. Salmi, *Design of Stainless Steel RHS Beams, Columns and beam-columns*, VTT Building Technology, Espoo, Finland, 1995.
- [4] P. J. Bredenkamp and G. van den Berg, "The strength of stainless steel built-up I-section columns," *Journal of Constructional Steel Research*, vol. 34, no. 2-3, pp. 131–144, 1995.
- [5] L. Wang, *Theoretical and Experimental Study on Stability of Thin-Walled Welded stainless Steel Tubular Axial Compression Members Andits Application in Space Grid structures*, Tianjin University, Tianjin, 1995.
- [6] J. Rhones, M. Macdonald, and W. Mcniff, "Buckling of cold-formed stainless steel columns under concentric and eccentric loading," in *Proceedings of the Fifteenth International Specialty Conference on Cold-Formed Steel Structures*, pp. 687–699, University of Missouri-Rolla, St. Louis, Missouri, USA, October 2000.
- [7] A. Tajia, *Test Report on Welded I and CHS Beams, Columns and beam-columns*, pp. 2–4, VTT Building Technology, Espoo, Finland, 1997.
- [8] J. Way and B. Burgan, *Report to ECSC -development of the Use of Stainless Steel in Construction: Structural Design of Stainless Steel Circular Hollow sections*, pp. 22–27, The Steel Construction Institute, Ascot, UK, 2000.
- [9] B. Young and W. Hartono, "Compression tests of stainless steel tubular members," *Journal of Structural Engineering*, vol. 128, no. 6, pp. 754–761, 2002.
- [10] Y. Liu and B. Young, "Buckling of stainless steel square hollow section compression members," *Journal of Constructional Steel Research*, vol. 59, no. 2, pp. 165–177, 2003.
- [11] L. Gardner and D. A. Nethercot, "Experiments on stainless steel hollow sections-Part 1: material and cross-sectional behaviour," *Journal of Constructional Steel Research*, vol. 60, no. 9, pp. 1291–1318, 2004.
- [12] L. Gardner and D. A. Nethercot, "Experiments on stainless steel hollow sections-Part 2: member behaviour of columns and beams," *Journal of Constructional Steel Research*, vol. 60, no. 9, pp. 1319–1332, 2004.
- [13] B. Young and W. M. Lui, "Tests of cold-formed high strength stainless steel compression members," *Thin-Walled Structures*, vol. 44, no. 2, pp. 224–234, 2006.
- [14] J. Becque, *The Interaction of Local and Overall Buckling of Cold-Formed Stainless Steel columns*, University of Sydney, Sydney, Australia, 2008.
- [15] M. Theofanous, T. M. Chan, and L. Gardner, "Structural response of stainless steel oval hollow section compression members," *Engineering Structures*, vol. 31, no. 4, pp. 922–934, 2009.
- [16] L. Gardner, "The use of stainless steel in structures," *Progress in Structural Engineering and Materials*, vol. 7, no. 2, pp. 45–55, 2005.
- [17] J. F. Xu and B. Li, "Discussion on the sustainability of stainless steel applied in architecture," *Advanced Materials Research*, vol. 476-478, pp. 1553–1556, 2012.
- [18] M. F. Hassanein and O. F. Kharoob, "Analysis of circular concrete-filled double skin tubular slender columns with external stainless steel tubes," *Thin-Walled Structures*, vol. 79, pp. 23–37, 2014.
- [19] Y. L. Li, X. L. Zhao, R. Raman Singh Raman Singh, and S. Al-Saadi, "Tests on seawater and sea sand concrete-filled CFRP, BFRP and stainless steel tubular stub columns," *Thin-Walled Structures*, vol. 108, pp. 163–184, 2016.
- [20] K. Khate, M. L. Patton, and C. Marthong, "Structural behaviour of stainless steel stub column under axial compression: a FE study," *International Journal of Steel Structures*, vol. 18, no. 5, pp. 1723–1740, 2018.
- [21] J. Ye, F. J. Meza, I. Hajirasouliha, and J. Becque, "Experimental investigation of cross-sectional bending capacity of cold-formed steel channels subject to local-distortional buckling interaction," *Journal of Structural Engineering*, vol. 145, no. 7, pp. 1–15, 2019.
- [22] B. F. Zheng, *Theoretical and Experimental Investigations on Cold-Formed Stainless Steel Columns and Beam columns*, Southeast University, Nanjing, China, 2020.
- [23] Z. Y. Fang, K. Roy Roy, J. Mares Mares, B. Sham, J. B. Chen, and J. B. P. Lim, "Deep learning-based axial capacity



- prediction for cold-formed steel channel sections using deep belief network,” *Structures*, vol. 33, pp. 2792–2802, 2021.
- [24] M. M. Seyed, H. Iman, and Y. Jun, “Optimisation of cold-formed steel beams for best seismic performance in bolted moment connections,” *Journal of Constructional Steel Research*, vol. 181, pp. 106621–106626, 2021.
- [25] Z. Y. Fang, K. Roy, Q. Ma, A. Uzzaman, and J. B. Lim, “Application of deep learning method in web crippling strength prediction of cold-formed stainless steel channel sections under end-two-flange loading,” *Structures*, vol. 33, pp. 2903–2942, 2021.
- [26] B. Chen, K. Roy, Z. Fang, G. Uzzaman, J. B. Raftery, and J. B. P. Lim, “Moment capacity of back-to-back cold-formed steel channels with edge-stiffened holes, un-stiffened holes, and plain webs,” *Engineering Structures*, vol. 235, pp. 112042–112050, 2021.
- [27] The European Union, *EN 1993-1-4 Eurocode 3: Design of Steel Structures: Part 1-4: General Rules-Supplementary Rules for Stainless Steels*, European Committee for Standardization, Brussels, Belgium, 2006.
- [28] Sei/Asce-8-02, *Specification for the Design of Cold-Formed Stainless Steel Structural members*, American Society of Civil Engineers, Reston, Virginia, 2002.
- [29] K. J. R. Rasmussen Rasmussen and J. Rondal, “Explicit Approach to design of stainless steel Columns,” *Journal of Structural Engineering*, vol. 123, no. 7, pp. 857–863, 1997.
- [30] P. Hrandil, L. Fulop, and A. Talja, “Global stability of thin-walled ferritic stainless steel members,” *Thin-Walled Structures*, vol. 61, no. SI, pp. 106–114, 2012.
- [31] 50068—2001, *Unified Standard for Reliability Design of Building structures*, China Architecture & Building Press, Beijing, China, 2001.
- [32] GB 50018—2002, *Technical Code of Cold-Formed Thin-wall Steel structures*, China Planning Press, Beijing, China, 2002.
- [33] GB 50017—2003, *Code for Design of Steel structures* China Planning Press, Beijing, China, 2003.
- [34] GB/T 4237—2007, *Hot Rolled Stainless Steel Plate, Sheet and Strip* China Standard Press, Beijing, China, 2007.
- [35] D. Fernando, J. G. Teng, W. M. Quach, and L. De Waal, “Full-range stress-strain model for stainless steel alloys,” *Journal of Constructional Steel Research*, vol. 173, pp. 106266–106270, 2020.
- [36] L. Gardner and M. Theofanous, “Discrete and continuous treatment of local buckling in stainless steel elements,” *Journal of Constructional Steel Research*, vol. 64, no. 11, pp. 1207–1216, 2008.
- [37] R. Hongthong, A. Benchaphong, and S. Benchanukrom, “Experimental and Theoretical study on screwed Connections in Cold-formed steel structure,” *Engineering Transactions*, vol. 67, no. 4, pp. 557–577, 2019.
- [38] Y. Li, G. Li, and Z. Shen, “Design reliability analysis of cold-formed thick-walled-steel members under axial compression,” *Journal of Building Structures*, vol. 36, no. 5, pp. 8–17, 2015.
- [39] GB 50009—2001, *Loadcode for the Design of Building structures*, China Architecture & Building Press, Beijing, China, 2002.
- [40] X. J. Tong, Q. Ma, and C. T. Wu, “A new method for solving equations of reliability index with JC method,” *Journal of Hebei Institute of technology*, vol. 25, no. 4, pp. 171–175, 2003.
- [41] GB/T 3280—2007, *Cold Rolled Stainless Steel Plate, Sheet and Strip* China Standard Press, Beijing, China, 2007.
- [42] The European Union, *EN 1993-1-1 Eurocode 3: Design of Steel Structures: Part 1-1: General Rules and Rules for Buildings*, European Committee for Standardization, Brussels, Belgium, 2006.